Performance Analysis of Limited-Range Wavelength Conversion in an OBS Switch

Vishwas S Puttasubbappa and Harry G Perros
{vsputtas,hp}@csc.ncsu.edu

Computer Science Department
North Carolina State University
Box 8206, Office 460 EGRC
1010 Main Campus Drive
Raleigh, NC 27695-7534

Abstract

We compute analytically burst blocking probabilities in an OBS switch when limited-range wavelength conversion is employed. Two separate queueing models are proposed and analyzed approximately; one for the case where the degree of conversion d is 1 or 2, another for large values of d. The arrival process of bursts is assumed to be an IDLE-ON process. The accuracy of these queueing models was tested against simulation. We show numerically that in order to keep the burst blocking probability within an acceptable level, the utilization of each wavelength has to be low.

1 Introduction

Optical Burst Switching (OBS) is one of the promising technologies to realize the next generation all-optical Internet, see Battestilli and Perros [4], Baldine et al [10], and Wei and McFarland [17]. Key features of OBS that makes it an attractive technology are the promise of high throughput and utilization, absence of O/E/O conversion for data bursts, absence of or limited usage of optical buffer at the core switches and being better suited for transmission of bursty traffic. OBS being placed between circuit switching and packet switching technologies imbibes the plus points from either of them and is also more likely to be implemented with the present state of physical device technologies.

In OBS, a control packet is transmitted ahead of an aggregation of data packets called the data burst by an *offset* amount of time. The control packet reserves resources at the core switches for the oncoming data burst. Several control packets may arrive at different input ports

of a switch at the same time and heading to the same output port. This leads to contention for resource possession (for eg: wavelength assignment at the output port). In case a control packet cannot reserve resources for its oncoming data burst, the data burst gets dropped. There are *three* techniques to minimize the above contention problem. They are *wavelength conversion*, use of *Fiber Delay Line (FDL) buffers* and *deflection routing*. A combination of these three techniques can also be employed to reduce blocking of data bursts. In the wavelength conversion technique, if the destination wavelength in the destination port is assigned to a different burst for that particular time interval, a wavelength converter is used to convert the data burst onto a different wavelength at the same fiber, if such a wavelength and a free converter is available. In the FDL buffer technique, an optical buffer in the form of an FDL can be used to delay bursts involved in contention and then transmitted through their original destination wavelength. In the third technique, deflection routing which involves transmitting a burst through a different fiber than the intended original destination fiber is employed to resolve contention, see Hsu et al [7]. Both the deflected burst and its control packet then have to find a different route other than their intended original route. The offset might also have to be recalculated because of the route change. A combination of these three techniques can also be employed to further reduce contention and thus blockage of data bursts. Gauger [6] examined the performance of OBS nodes which employ wavelength converter pools and FDL buffers for contention resolution. Several strategies based on different ordering of probing converter pools and FDL buffers have been proposed to optimize performance such as minimizing delay or the number of converters.

In this paper, we focus on wavelength conversion to reduce contention among data bursts. We consider only the case of limited-range wavelength conversion. In limited-range wavelength conversion, a burst arriving on a wavelength can be converted to a fixed set of wavelengths above and below the original wavelength. The degree of conversion d defines the number of wavelengths on either side of the original wavelength. Thus, an incoming data burst can be converted to a total of $(2 * d + 1)$ destination wavelengths. Yates et al [5] were the first to model a system with limited-range wavelength conversion. Until then, all the papers assumed full-range wavelength conversion. In [5], the all-optical translators considered were based on four-wave mixing in Semiconductor Optical Amplifiers (SOA). A model was developed to analyze the blocking performance of two-hop and multiple-hop paths in unidirectional ring and mesh-torus networks. They also stated that almost all of the network performance gained by full-range conversion can be attained by half the number of converters employing limited-range wavelength conversion. Tripathi and Sivarajan [14] developed an analytical model for fixed routing of lightpaths which can be applied to any topology. They stated that the benefits of full-range wavelength conversion could be achieved by limited-range conversion with degree of conversion being only 1 or 2. Rosberg et al [16] proposed a framework to compute the path blocking probabilities in an OBS network. They showed that for OBS networks, even a small degree of conversion can bring about significant reduction in blocking. However, they also showed

that for OBS networks, unlike previous studies which are based on acknowledgement-based networks, full-range conversion resulted in significantly less blocking probabilities than limited-range wavelength conversion with small degree of conversion. The proposed framework used a generalized form of the Erlang fixed-point approximation. Akar and Karasan [2] proposed a method to exactly calculate the blocking probabilities in an OBS switch with partial wavelength conversion, i.e number of converters available being less than the number of wavelengths. A numerical method was used to solve the underlying continuous time Markov process. They also showed that their method could be used to efficiently calculate blocking probabilities for very large number of wavelengths.

Previous studies in OBS which dealt with limited-range wavelength conversion focused on computing link blocking probabilities and path blocking probabilities, see Rosberg et al [16]. They also assumed Poisson arrivals for their model. In this paper, we focus on a single OBS switch and we assume sources to be of ON-OFF nature.

We develop an analytical model to determine the blocking probabilities for bursts in a core OBS switch which employs limited-range wavelength conversion to resolve contention among bursts. We assume the absence of FDLs and deflection routing. The blocking probabilities obtained from this queueing model are approximate. We propose a product-form solution from which blocking probabilities can be computed for large number of wavelengths, w, but only for $d = 1, 2$. We then develop a large scale approximation technique which can be applied to large values of w and d.

The paper is organized as follows: Section 2 describes the architecture of the core OBS switch that we have assumed for our model. In Section 3, we present an approximate queueing model for limited-range wavelength conversion for the case of small d. In Section 4, we describe an approximate model for large w and d. In Section 5, we compare the outputs of our analytical models with simulation results, and in Section 6, we draw conclusions.

2 The switch

The components of a core OBS switch we use in our model are depicted in figure 1. The switch is comprised of k incoming and k outgoing fibers, the switching fabric and wavelength converters. Such a switch can be implemented using several architectures, see for instance Xiong et al [15], Qin and Yang [12], and Ramamirtham and Turner [13]. Each output fiber has a set of wavelength converters, c, that can be used by bursts traveling out of that particular fiber. The bandwidth in each fiber is partitioned into several wavelengths, w, using Wavelength Division Multiplexing (WDM).

In this paper, we only model a single output fiber with its own set of wavelength converters. Each outgoing wavelength l_i, $i = 1, 2, \ldots, w$, has k number of incoming wavelengths, l_i, one per

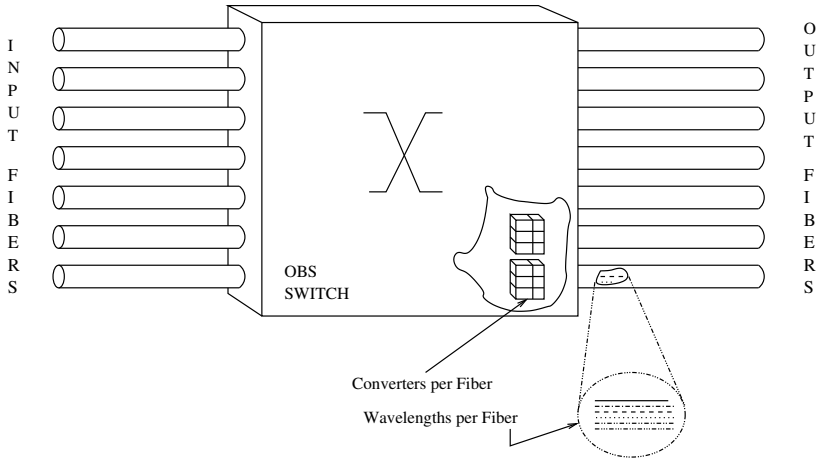

Figure 1: Switch Architecture

input fiber, targeted into it. Part of the bursts arriving in each of the k input wavelengths l_i, is switched to the destination wavelength l_i of the output fiber under study. The remaining bursts are switched through other output fibers. An incoming burst on l_i will try to be scheduled on its *home* wavelength l_i in the outgoing fiber. In case the home wavelength is busy, the burst tries to occupy adjacent wavelengths in the range $(l_i - d, l_i + d)$, if a converter in the common converter pool per output fiber is available. The method of trying to occupy an alternate wavelength within the range $(l_i - d, l_i + d)$ will be explained in the analytical model section.

3 The Queueing model for small d

Let us consider the birth-death process for limited-range wavelength conversion shown in figure 2. The figure shows all the possible transitions for a system consisting of 3 wavelengths with $d = 1$ and $c = w$. A Poisson arrival process to each wavelength is assumed with a rate λ. A burst arriving on the middle wavelength can be converted to either ones on its side provided they are free. For the border wavelengths, the bursts can undergo wavelength conversion only to the middle wavelength. Each state is depicted by (S_i, S_j, S_k), where S_x is either 0 or 1, indicating the occupancy of the server x. The Markov process is governed by the following set of equations:

$$3\lambda P_{000} = \mu P_{100} + \mu P_{010} + \mu P_{001}$$

$$(2\lambda + \mu) P_{001} = \lambda P_{000} + \mu P_{101} + \mu P_{011}$$

$$(2\lambda + \mu) P_{010} = \lambda P_{000} + \mu P_{110} + \mu P_{011}$$

$$(\lambda + 2\mu) P_{011} = \lambda P_{010} + \mu P_{111} + \lambda P_{001}$$

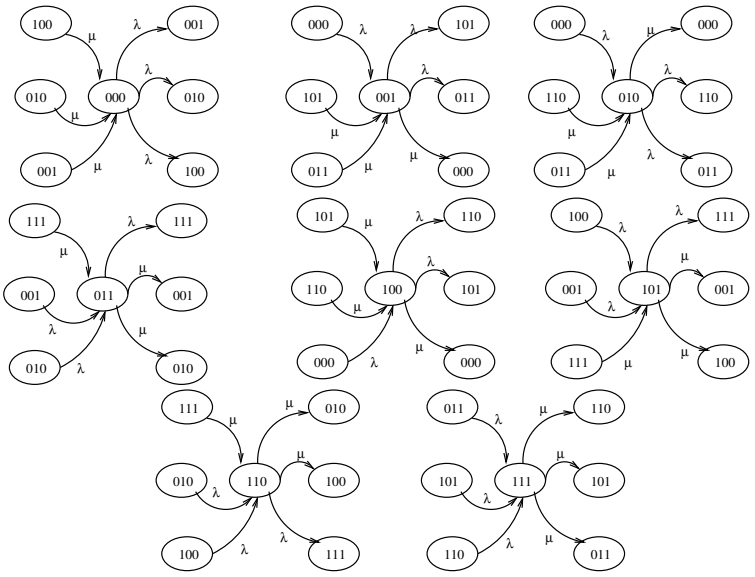

Figure 2: Birth-Death process for limited-range conversion ($w = 3, c = 3, d = 1$)

$$(2\lambda + \mu)P_{100} = \mu P_{110} + \mu P_{101} + \lambda P_{000}$$

$$(\lambda + 2\mu)P_{101} = \lambda P_{100} + \lambda P_{001} + \mu P_{111}$$

$$(\lambda + 2\mu)P_{110} = \lambda P_{100} + \lambda P_{010} + \mu P_{111}$$

$$3\mu P_{111} = \lambda P_{110} + \lambda P_{101} + \lambda P_{011}$$

It can be seen that the above equations do not satisfy local balance. Thus, the Markov process for limited-range wavelength conversion does not have a product-form solution. In view of this, we propose a queueing model with simultaneous resource possession which is solved approximately in order to compute the blocking probabilities in an OBS switch with limited-range wavelength conversion.

Let us consider an example with $w = 3$, $c = 3$ and $d = 1$. Figure 3 depicts the decomposition of this system with $w = 3$ and $d = 1$ into three sub-systems $\overline{n}_1$,$\overline{n}_2$ and $\overline{n}_3$ each being an Erlang loss queue. The number of sub-systems is equal to the number of wavelengths w. Each sub-system $\overline{n}_i$ has a *home* wavelength λ_i and neighboring wavelengths into which a burst coming on the home wavelength can be converted into. We represent each wavelength with a server. Thus, the number of servers in each sub-system ranges from $(d + 1)$ to $(2 * d + 1)$. The border sub-systems $\overline{n}_1$ and $\overline{n}_3$ have two servers and the central sub-system $\overline{n}_2$ has three servers. The state of each server is represented by $n_{i,j} \epsilon \{0, 1\}$, where i is the sub-system and j is the wavelength. Thus, $\overline{n}_1 = \{n_{1,1}, n_{1,2}\}$, $\overline{n}_2 = \{n_{2,1}, n_{2,2}, n_{2,3}\}$ and $\overline{n}_3 = \{n_{3,2}, n_{3,3}\}$.

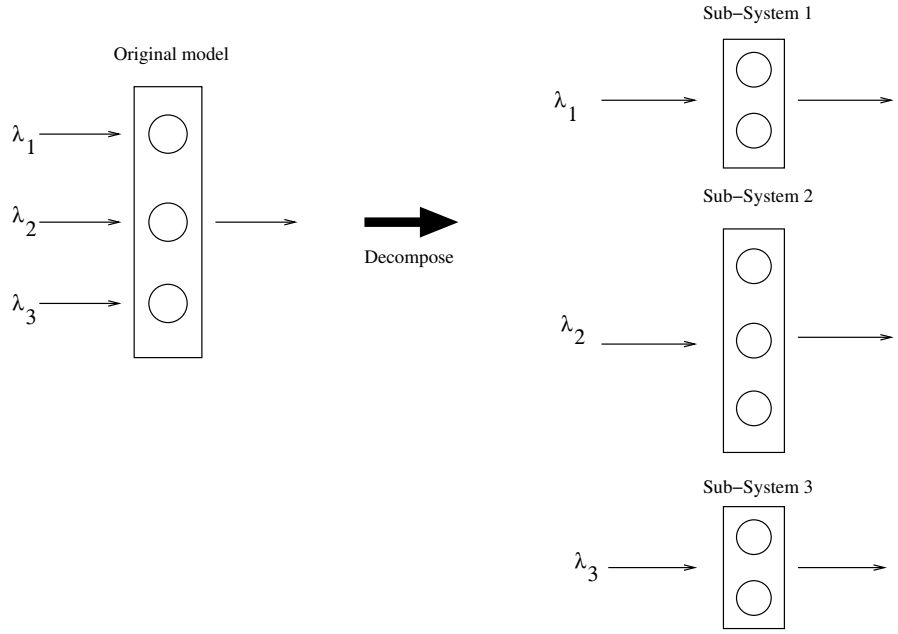

Figure 3: A three node model

The state of the system is given by the union of states of servers in all the sub-systems combined. Thus, for the three node example, the state of the system is represented by the tuple $(\overline{n}_1, \overline{n}_2, \overline{n}_3) = (n_{1,1}, n_{1,2}, n_{2,1}, n_{2,2}, n_{2,3}, n_{3,2}, n_{3,3})$.

Let $p(\overline{n}_1, \overline{n}_2, \overline{n}_3)$ be the probability of the system being in one such state. Then, we have

$$p(\overline{n}_1, \overline{n}_2, \overline{n}_3) = \frac{1}{G} * p(\overline{n}_1) * p(\overline{n}_2) * p(\overline{n}_3) \tag{3.1}$$

or,

$$p(n_{1,1}, n_{1,2}, n_{2,1}, n_{2,2}, n_{2,3}, n_{3,2}, n_{3,3}) = \frac{1}{G} * p(n_{1,1}, n_{1,2}) * p(n_{2,1}, n_{2,2}, n_{2,3}) * p(n_{3,2}, n_{3,3}) \tag{3.2}$$

where $G = \sum p(\overline{n}_1) * p(\overline{n}_2) * p(\overline{n}_3)$ summed over all feasible states.

The set of feasible states is computed using the following two rules:
Rule 1: A wavelength server can be occupied in only one sub-system
Rule 2: The number of conversions cannot exceed c
Thus we have the following constraints:

$$n_{1,1} + n_{2,1} = 1 \tag{3.3}$$

$$n_{1,2} + n_{2,2} + n_{3,2} = 1 \tag{3.4}$$

$$n_{2,3} + n_{3,3} = 1 \tag{3.5}$$

$$n_{1,2} + n_{2,1} + n_{2,3} + n_{3,2} \leq c \tag{3.6}$$

The wavelength occupancy constraint (*Rule 1*) and the converters constraint (*Rule 2*) reduce the state space from which the solution is computed. The computation of the individual subsystem probabilities $p(\overline{n}_x)$, where $x\epsilon\{1 \ldots w\}$ will be explained in the sub-section 3.2.

When we generalize our model to any number of wavelengths w, we have,

$$p(\overline{n}_1, \overline{n}_2, \overline{n}_3, \ldots, \overline{n}_w) = \frac{1}{G} * p(\overline{n}_1) * p(\overline{n}_2) * p(\overline{n}_3) * \ldots * p(\overline{n}_w) \tag{3.7}$$

The model is further decomposed so as to include the constraints of wavelength occupancy and the number of available converters. Each subsystem thus becomes:

$$\overline{n}_i = (n_{i,i-d}, n_{i,i-d+1}, ..., n_{i,i}, ..., n_{i,i+d-1}, n_{i,i+d}) \tag{3.8}$$

and in $n_{i,j}$, i,j $\epsilon\{1 \ldots w\}$

We have the following constraints:

$$n_{i,i-d} + n_{i,i-d+1} + \ldots + n_{i,i-1} + n_{i,i} + n_{i,i+1} + \ldots + n_{i,i+d-1} + n_{i,i+d} = 1 \forall i \epsilon (1 \ldots w) \tag{3.9}$$

$$\sum_{i=1, j=i-d, j\geq 1}^{i=w, j=i+d} n_{i,j} \leq c \tag{3.10}$$

We note that the approach described above is similar in spirit to the analysis of circuit-switched networks, see for instance Alnowibet and Perros [3]. The computation of G is a complicated task because of the state space explosion with large values of w and d. We shall describe the approach we take for the computation of G in sub-section 3.3. Once the probability of the system existing in each state has been determined, the blocking probability of each wavelength is then the sum of all the corresponding blocking states.

3.1 The Arrival process

We use the IDLE-ON arrival process shown in figure 4 to generate bursts on a single incoming wavelength l_i. The IDLE and ON periods are exponentially distributed with a mean of $\frac{1}{\nu}$ and $\frac{1}{\mu}$ respectively. A single ON period generates a single burst. An IDLE period is followed by the ON period and vice-versa. If a burst is dropped, the source returns to the IDLE state. Since there are k input fibers, the burst arrival process from all the k incoming wavelengths l_i is the superposition of k single IDLE-ON sources as shown in figure 4(b). We assume that all the k arrival IDLE-ON sources are identical.

As described in section 2, we are modeling a single output fiber. Each wavelength in the fiber will only have some of the traffic directed towards it from its k corresponding input wavelengths.

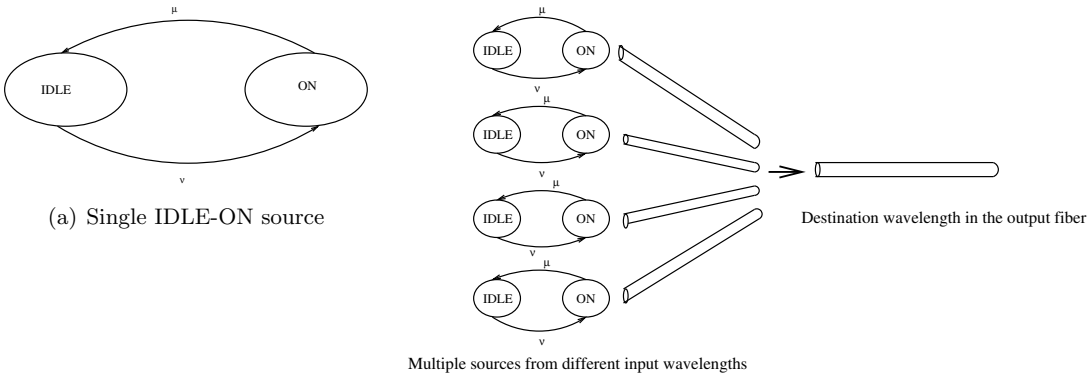

(a) Single IDLE-ON source

(b) Multiple IDLE-ON sources

Figure 4: Arrival process

Consequently, the IDLE period is assumed to have been appropriately extended so that only the bursts destined to the outgoing wavelength in the fiber are modeled. In this paper, we assume that the appropriately extended IDLE period is given.

3.2 Computing the state probabilities for each sub-system

Figure 5 depicts the birth-death process for a single sub-system. The sub-system has 3 wavelengths with degree of conversion $d = 1$, $c = 3$ and the arrival process is assumed to be Poisson. On arrival, a data burst tries to occupy the middle wavelength which is its home wavelength. If the home wavelength is busy, with equal probability the burst tries to occupy one of the adjacent wavelengths. The following set of equations govern the process.

$$\lambda P_{000} = \mu P_{100} + \mu P_{010} + \mu P_{001}$$

$$(\lambda + \mu) P_{001} = \mu P_{101} + \mu P_{011}$$

$$(\lambda + \mu) P_{010} = \lambda P_{000} + \mu P_{110} + \mu P_{011}$$

$$(\lambda + 2\mu) P_{011} = \lambda/2 P_{010} + \mu P_{111} + \lambda P_{001}$$

$$(\lambda + \mu) P_{100} = \mu P_{110} + \mu P_{101}$$

$$(\lambda + 2\mu) P_{101} = \mu P_{111}$$

$$(\lambda + 2\mu) P_{110} = \lambda P_{100} + \lambda/2 P_{010} + \mu P_{111}$$

$$3\mu P_{111} = \lambda P_{110} + \lambda P_{101} + \lambda P_{011}$$

The state probabilities can be derived from the above set of equations and it does not have a closed-form expression. On increasing the values of w and d, it gets difficult to solve a Markov

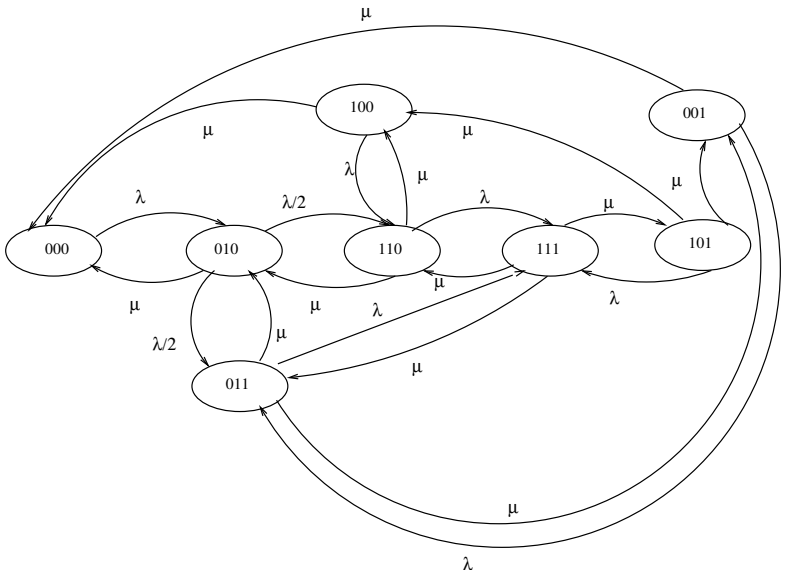

Figure 5: Birth-Death process for a single sub-system ($w = 3, c = 3, d = 1$)

chain for each sub-system. We note that if we assume that on arrival a burst occupies any free server randomly selected, the above system becomes an Erlang or an Engset system depending on whether we assume a Poisson or IDLE-ON arrival process. This gives rise to a product-form solution which is an approximation to the probability terms $p(n_x)$ in equation 3.7.

In equation 3.2, the probability terms on the right hand side are determined using the Engset model. If n is the number of servers, k the number of input fibers and μ, ν are as described in the arrival process, the probability that there are i customers in such a $M/M/n/n/k$ system is given by:

$$\pi_i^* = \frac{\binom{k-1}{i}(\frac{\nu}{\mu})^i}{\sum_{j=0}^{n}\binom{k-1}{j}(\frac{\nu}{\mu})^j} \tag{3.11}$$

The state probabilities given by equation 3.11 are those as seen by an arrival.

The probability that a specific set of i servers is occupied in a sub-system is given by:

$$\pi_i = \frac{\pi_i^*}{\binom{n}{i}} \tag{3.12}$$

The product of such probability terms for all sub-systems, if the state is valid, can be added to compute G, see equation 3.7. The blocking probability of a particular wavelength is finally computed by summing up all the appropriate blocking states.

3.3 Computation of G

We now describe the approach taken to compute the normalization constant G.

Let us construct a resource allocation matrix to represent the sub-systems. An example of such a matrix is shown in figure 6, assuming that $w = 7$ and $d = 1$. The matrix shows the wavelengths represented in each sub-system indicated by the symbol $\surd$. There are as many sub-systems as the number of wavelengths. The symbol $\surd$ assumes the value of 1 if the wavelength is used in the corresponding sub-system. Otherwise, it is zero. Thus, each column can have a single 1. Further, to impose the number of converters constraint, the sum of all non-diagonal elements cannot exceed the number of available converters. Using this matrix, it is easy to visualize the state space constraints 3.9 and 3.10.

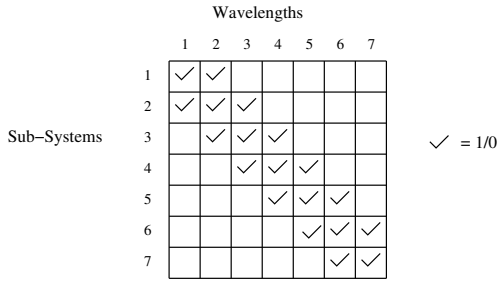

Figure 6: Resource Allocation Matrix

By brute-force enumeration, it takes $O(w^w)$ to cover the entire state space and determine the blocking probabilities for each wavelength. It is clear that brute-force enumeration cannot be used to compute G for large values of w and d. This approach can be used for $d = 1, 2$ and very small values of w. For larger values of d, we propose the *large scale approximation technique* described in section 4.

3.4 Large number of wavelengths

In this section, we describe a method for computing the blocking probabilities for large number of wavelengths, and $d = 1, 2$.

As was described in section 3.3, we can compute G by brute-force enumeration only for very low values of d and w. However, there are some properties of the blocking probabilities with increasing number of wavelengths that we can make use of in order to compute blocking probabilities for these large systems.

Figure 7 plots the simulation results for the blocking probability of the middle wavelength with increasing number of w in the system. The number of converters is set to 33% of the

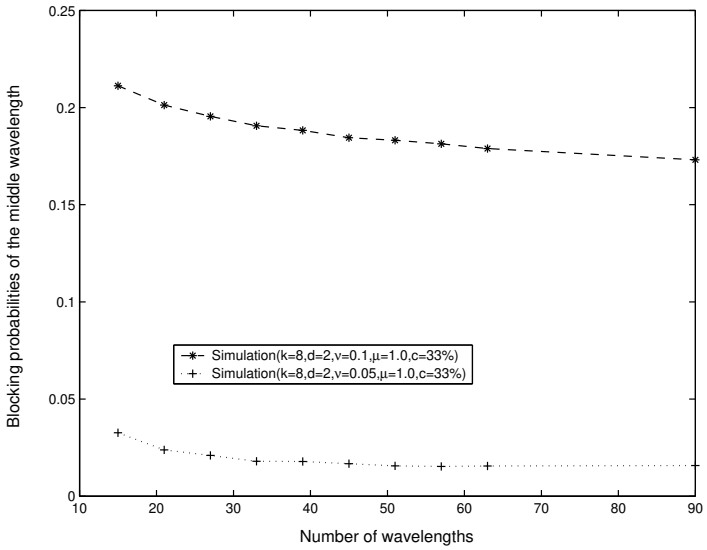

Figure 7: Proportional use of converters

number of wavelengths and it increases proportionally with the number of wavelengths. It can be seen that with increase of w, there is a very small gradual decrease in the blocking probability. It can also be seen that the trend is similar for different arrival rates. We assume an identical superimposed arrival process to each wavelength.

Figure 8 plots the simulation results for the blocking probabilities for all the wavelengths in the system, for two different cases. We assume that each wavelength is fed by the same superposition arrival process. It can be seen that the border wavelengths have the highest blocking since the degree of conversion is smaller for them compared to the center wavelengths. In the following sections, we focus only on the blocking probability of the middle wavelength. For a more detailed discussion on the blocking probabilities of all wavelengths in the spectrum, the reader is referred to appendix A of [11]. Here, we also assume symmetric traffic wherein each wavelength is fed by the same arrival process resulting in the same arrival rate.

3.5 The four-point method

Figure 9(a) gives another plot of the simulation results for the blocking probability of the middle wavelength with increasing number of wavelengths. It should be noted that the graphs in figures 7 and 9(a) represent the same trend, except that the range of system size w shown is different. When w is small, the blocking probabilities are extremely sensitive to the effect of lesser number of servers available for the border wavelengths. As w increases, this effect decreases rapidly initially and then gradually. These two trends can be seen in the figure 9(a) and only the

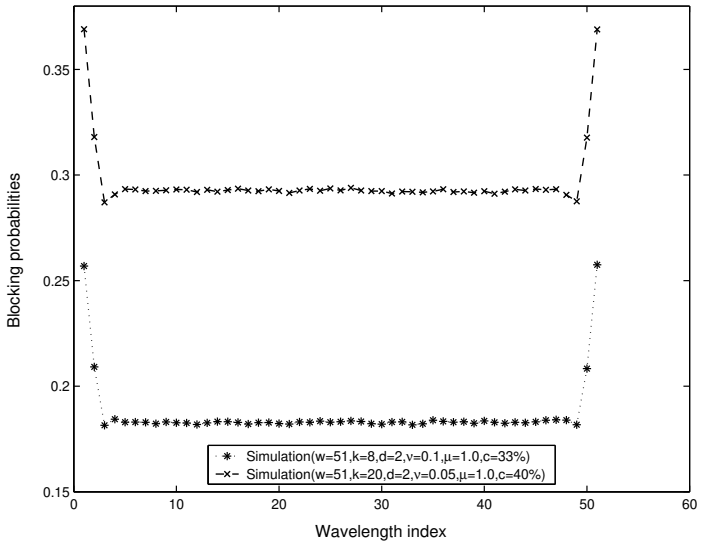

Figure 8: Blocking probabilities for each wavelength

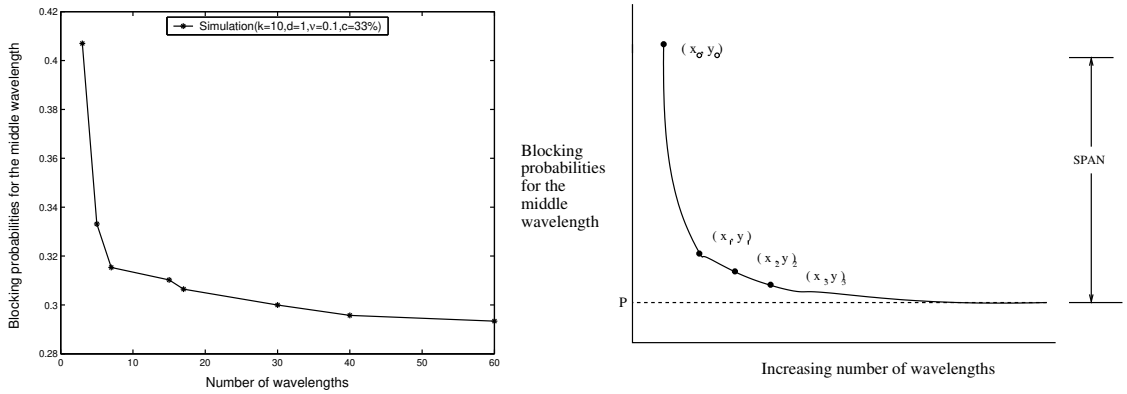

(a) Exponential decay

(b) Four-point method

Figure 9: Large number of wavelengths

gradual decrease can be seen in figure 7.

We note that from figure 9(a) that the distribution is very similar to the exponential distribution. In the four-point method, we use the brute-force enumeration described in section 3.3 to calculate the initial 4 points on the curve. We then use these points to determine the value of the plateau P of the curve, see figure 9(b).

Let $(x_0, y_0), (x_1, y_1), (x_2, y_2)$ and (x_3, y_3) be the initial 4 points on the curve. y_0, y_1, y_2 and y_3 can be calculated by brute force. The size of the systems is $(2*d+1)$, $(2*d+3)$, $(2*d+5)$ and $(2*d+7)$ respectively. A one phase exponential decay function with the initial 4 points is fitted (see Motulsky and Christopoulos [8]) from which the value of P, i.e the blocking probability for large number of w and for $d = 1, 2$, can be obtained.

4 Large scale approximation

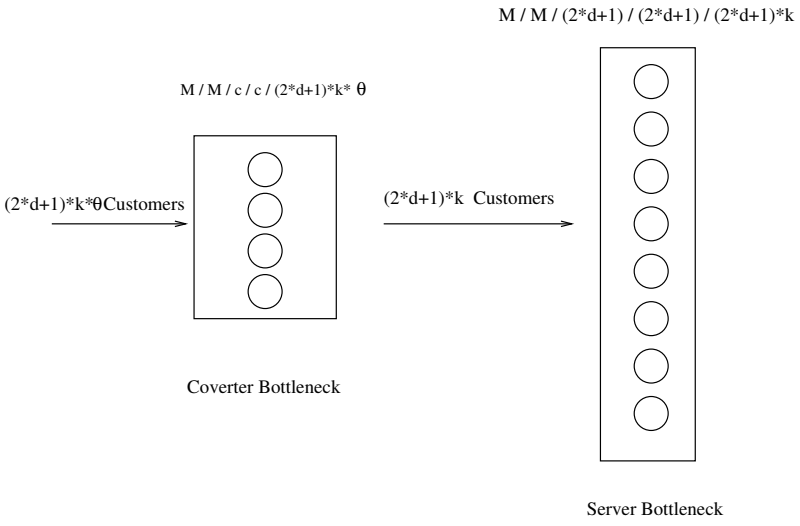

Figure 10: Large scale approximation

The methods discussed in section 3 can only be applied for $d = 1, 2$. In this section, we describe an approximate model for large d. The schematics of the model is as shown in figure 10.

The system is decomposed into two loss queues. The first one is referred to as the *server bottleneck* and the second one as the *converter bottleneck*. The server bottleneck queue is used to determine the blocking due to lack of servers, i.e. wavelengths, for a given d, and the converter bottleneck queue is used to determine blocking due to lack of converters for a given c. The server bottleneck and the converter bottleneck queues are analyzed separately and independence

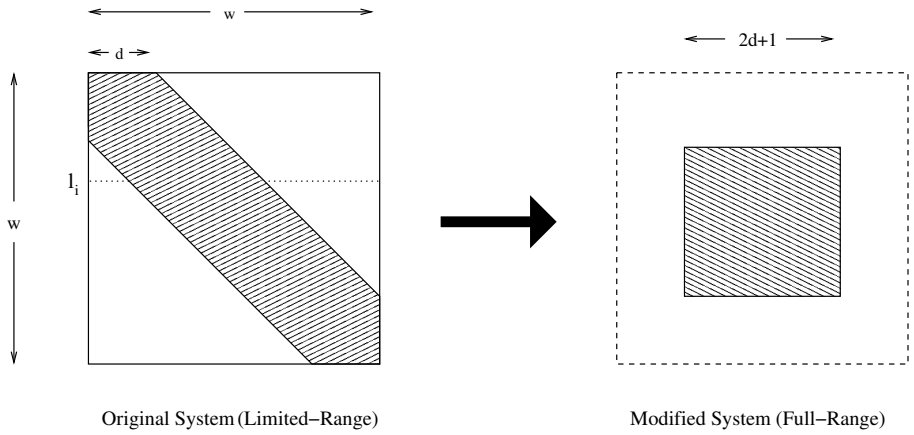

Figure 11: Transformation from limited-range conversion to full-range conversion

is assumed between them.

Figure 11 shows the transformation of the server bottleneck from limited-range conversion to full-range conversion. The figure on the left hand side is similar to the resource allocation matrix shown in figure 6. The group of $\surd$ symbols has been replaced by a band. A burst arriving on wavelength l_i can be converted into any wavelength within the band on its horizontal axis. Intuitively, it could be seen that if this band covered the complete square which results in full-range conversion, a lower bound could be achieved for the blocking probabilities. However, such a lower bound will not be very tight. Supposing, we consider a smaller system size for full-range conversion, the increase in blocking probabilities due to this system size transformation could be compensated by the decrease in blocking probabilities due to the transformation from limited-range conversion to full-range conversion. In essence, limited-range wavelength conversion for the entire number of wavelengths w can be modeled by full-range wavelength conversion for a smaller set of wavelengths. The blocking probabilities are thus approximate and only an *average blocking probability* can be determined with this approach. Such a system size was found to be close to $2 * d + 1$ wavelengths. The full-range conversion scenario is shown in the right hand part of figure 11. Simulation results of figure 12 confirms the validity of such a transformation. It has to be noted that the y axis denotes the average blocking probability of all the wavelengths. We use the same superposed arrival process to each wavelength as was described in section 3.1.

The server bottleneck queue is modeled by an Engset system $M/M/(2 * d + 1)/(2 * d + 1)/((2 * d + 1) * k)$. The converter bottleneck queue is also modeled as an Engset system. But the percentage of $(2 * d + 1) * k$ customers, θ, that have to use the converter pool needs to be determined. This can be determined approximately as follows. The probability that an arriving burst uses a converter is equal to the probability that the burst's wavelength is busy, which is equal to the blocking probability in an $M/M/1/1/k$ system, $p_{Blocking}(M/M/1/1/k)$. Therefore,

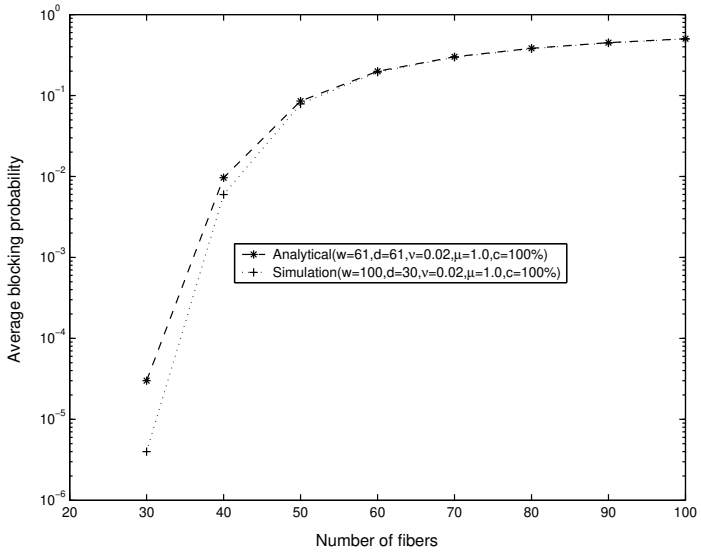

Figure 12: Full-range conversion

θ is set equal to $p_{Blocking}(M/M/1/1/k)$. Thus, the Engset system for the converter bottleneck becomes $M/M/c/c/\lceil(2*d+1)*k*\theta\rceil$.

Let p_{Bs} and p_{Bc} be the blocking probabilities at the server bottleneck queue and the converter bottleneck queue. Then, because of the independence assumption, the probability that a burst gets blocked is given by:

$$p_B = 1 - (1 - p_{Bs})(1 - p_{Bc}) \tag{4.13}$$

4.1 Case of No conversion and Full-range conversion cases

For the case of *no conversion*, the blocking probability of each wavelength is given by:

$$p_{No-conversion} = p_{Blocking}(M/M/1/1/k) \tag{4.14}$$

For *full-range conversion*, the blocking probability of each wavelength is given by:

$$p_{Full-range-conversion} = p_{Blocking}(M/M/w/w/(w*k)) \tag{4.15}$$

4.2 Utilization

As shown above, the server bottleneck queue and the converter bottleneck queue is each analyzed as an Engset system as shown in figure 13. The users will either be in the first set of servers (N of them) during which time they are idle. The users are busy when they are in the second

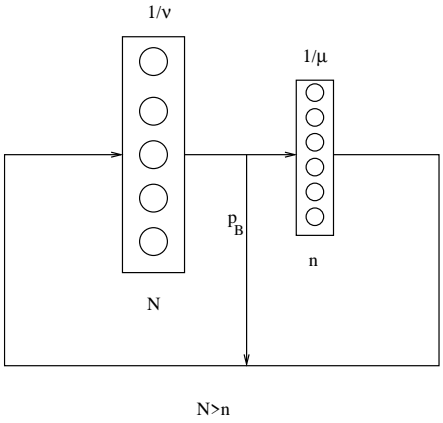

Figure 13: The Engset System

set of servers (n of them). The service rates are ν and μ for the first and second set of servers respectively. The probability that a user gets blocked at the second set of servers is p_B.

Let $p_1(i)$ and $p_2(i)$ be the probabilities of having i customers in the first and second set of servers respectively. Then, the server (or wavelength) utilization is:

$$\cup = (\frac{\lambda^*}{n})(\frac{1}{\mu})$$

where

$$\lambda^* = \lambda(1 - p_B)$$

and

$$\lambda = [\sum_{j=0}^{k} j * \nu * p_1(\#customers = j)]$$

Thus,

$$\cup = \frac{[\sum_{j=0}^{N} j * \nu * p_1(\#customers = j)] * (1 - p_B)}{n} * \frac{1}{\mu} \tag{4.16}$$

5 Results

An event based simulation model was constructed to evaluate the accuracy of the results of the analytical model. The simulation results were plotted with 95% confidence interval estimated by the method of batch means, see Perros [9]. Each batch is completed when every wavelength has 30,000 bursts arriving at it. The confidence intervals are very tight and are not discernible in the graphs. A software called *GraphPad Prism* [1] was used to fit a one phase exponential decay function with the initial 4 points as described in the four-point method.

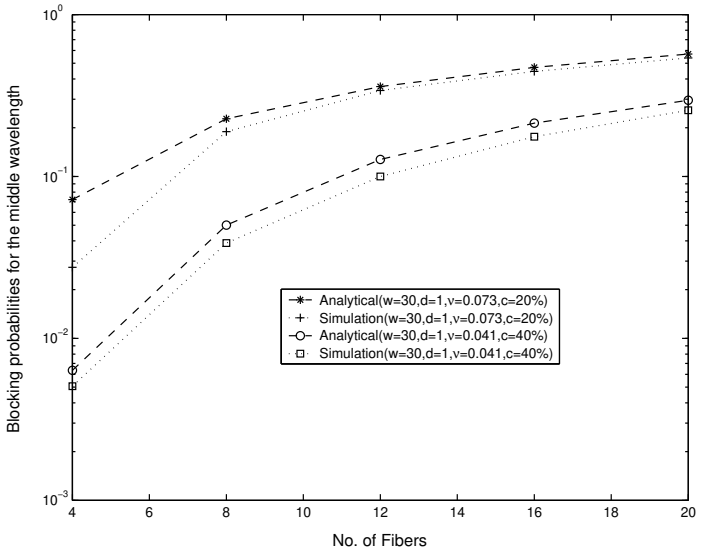

Figure 14: Blocking vs No. of Fibers for $d = 1$

The blocking probability of the center wavelength was calculated by varying ν (which varies the arrival rate), the number of fibers k, the degree of conversion d, and the number of wavelengths w. Both analytical results and simulation results have been plotted. We use the four-point method for $d = 1, 2$ and the large scale approximation for larger d.

Figure 14 plots the blocking probability of the middle wavelength with increasing number of fibers k for $w = 30$, $d = 1$, $\nu = 0.073$, $c = 20\%$ and $w = 30$, $d = 1$, $\nu = 0.041$, $c = 40\%$. The number of input wavelengths that can source traffic to a particular wavelength has to be greater than $2 * d + 1$ (condition for an Engset system). Thus, $k \geq 4$ in the graph. We observe that the analytical model provides higher blocking probabilities than the simulation results.

Figure 15 plots the blocking probabilities with increasing arrival rate (by increasing ν) for $w = 30$, $k = 8$, $d = 1$, $c = 20\%$ and $w = 30$, $k = 12$, $d = 1$, $c = 30\%$. Here too, it can be seen that the analytical values are above the simulation values.

In figures 16, 17 and 18, we plot the blocking probabilities for varying k, c and ν for $d = 2$. The way we take the initial 4 points differs for $d = 2$. To get the fourth point, we have to consider a system of size $(2 * d + 7) = 11$. By brute-force enumeration, it is not possible to explore all the states of such a system within reasonable time. So, we get the fourth point via simulation, which takes far lesser time. We note that the analytical values are much closer to the simulation ones than in the case of $d = 1$. However, the range for good values seem to be between 10^{-1} and 1.

We now plot the blocking probabilities for large values of d and w using the large scale

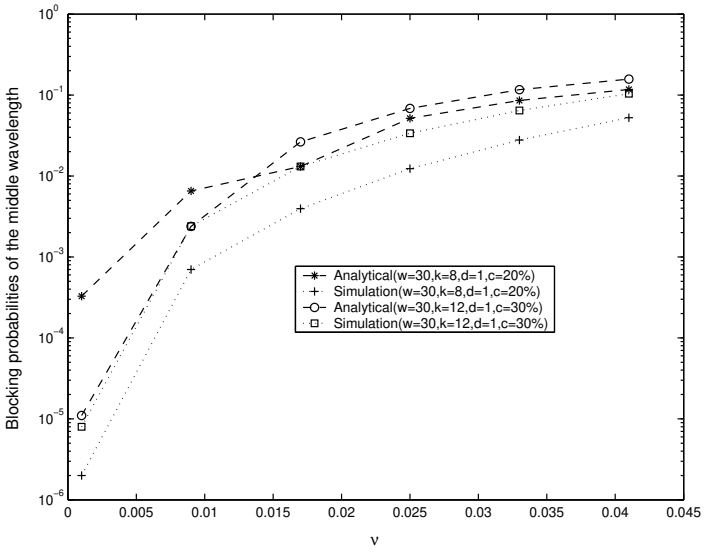

Figure 15: Blocking vs ν for $d = 1$

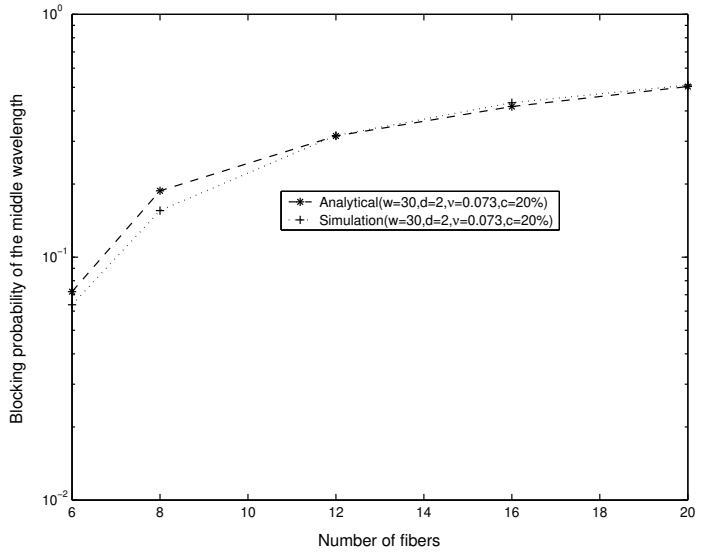

Figure 16: Blocking vs No. of Fibers for $d = 2$

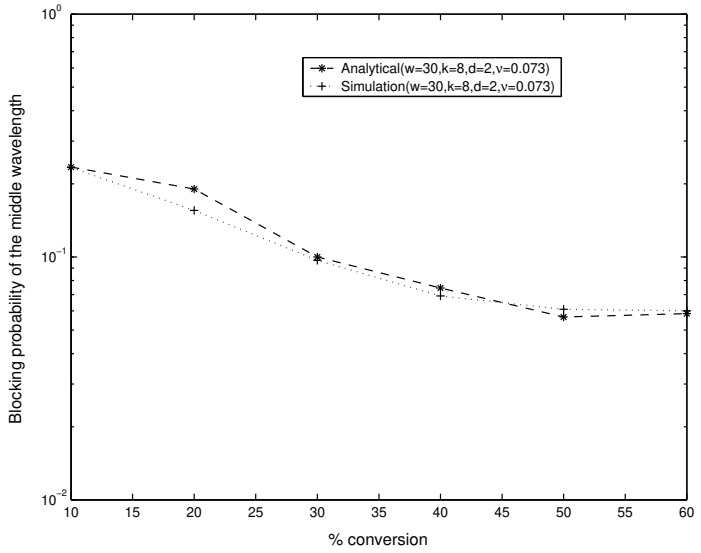

Figure 17: Blocking vs % conversion for $d = 2$

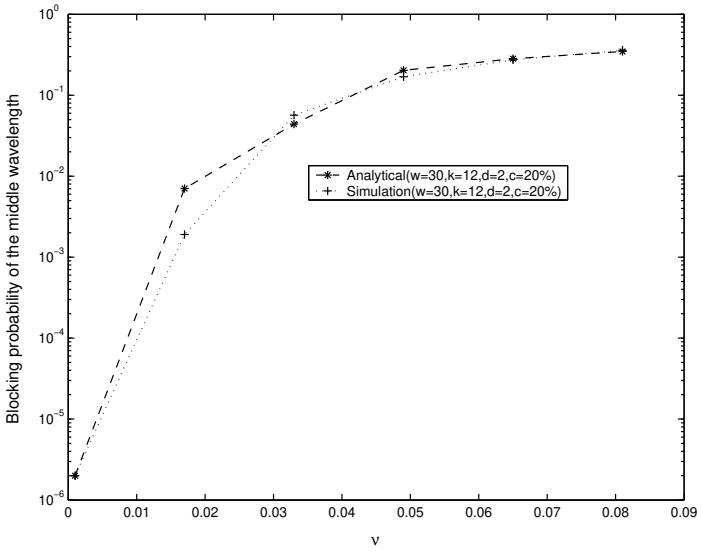

Figure 18: Blocking vs ν for $d = 2$

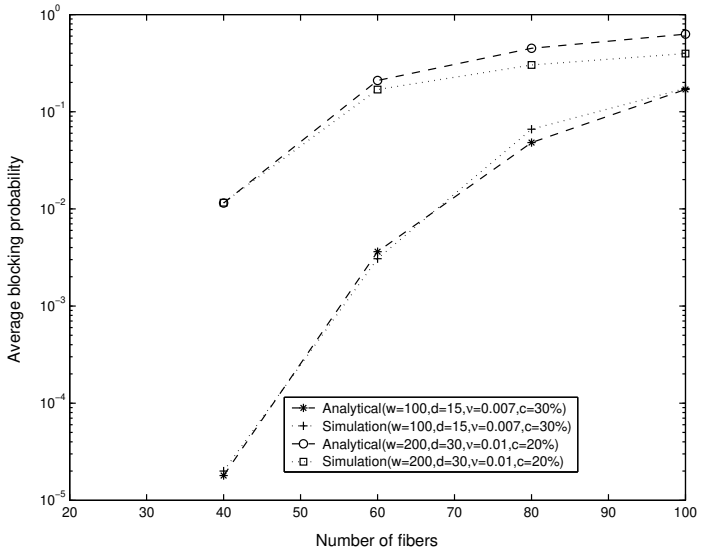

Figure 19: Blocking vs No. of Fibers for large systems

approximation method described in section 4.

Figure 19 plots the average blocking probability with increasing number of fibers ranging from 20 to 100 for $w = 100$, $d = 15$, $\nu = 0.007$, $c = 30\%$ and $w = 200$, $d = 30$, $\nu = 0.01$, $c = 20\%$. The average blocking probability is the sum of blocking probabilities of all the wavelengths divided by the number of wavelengths. It has to be noted that the large scale approximation technique of section 4 computes the average blocking probability. The analytical values are close to the simulation results.

Figures 20, 21, 22 plot the average blocking probability with increasing arrival rate (by increasing ν), increasing percentage of conversion, increasing degree of conversion d respectively.

As was mentioned for $d = 1, 2$, increasing d decreases the blocking probabilities when the probability range is very low. This also applies to large systems as can be seen from figure 22. Thus, increasing d is most effective at low blocking probabilities which can be due to low arrival rate and/or high percentage of conversion. After a certain value of d, larger values do not have an impact on blocking. In this case, it seems that blocking is predominantly due to the lack of converters.

Figure 23 plots the average blocking probability versus utilization for an outgoing wavelength. It can be seen that the link has to be run at very low utilization in order to have a low blocking probability.

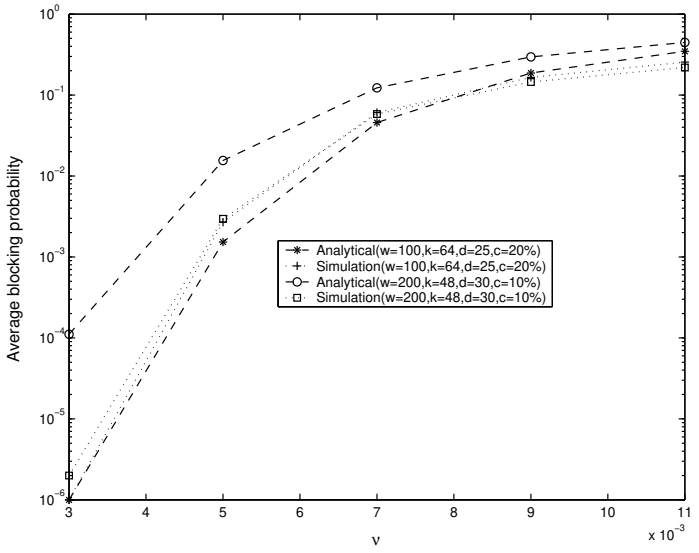

Figure 20: Blocking vs ν for large systems

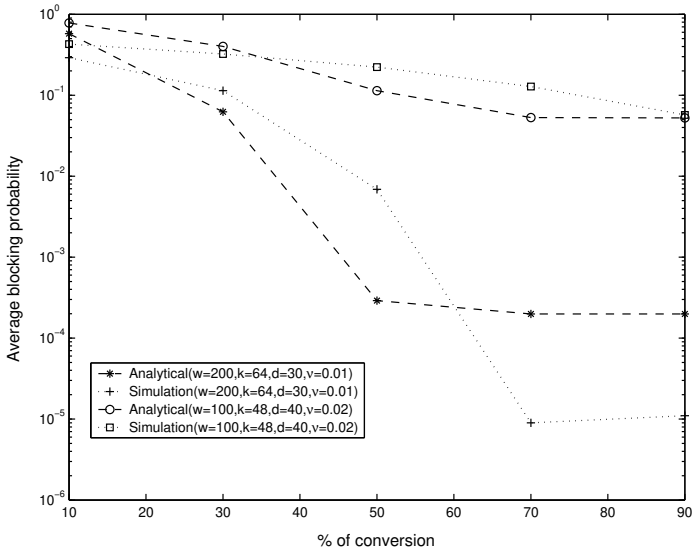

Figure 21: Blocking vs % conversion for large systems

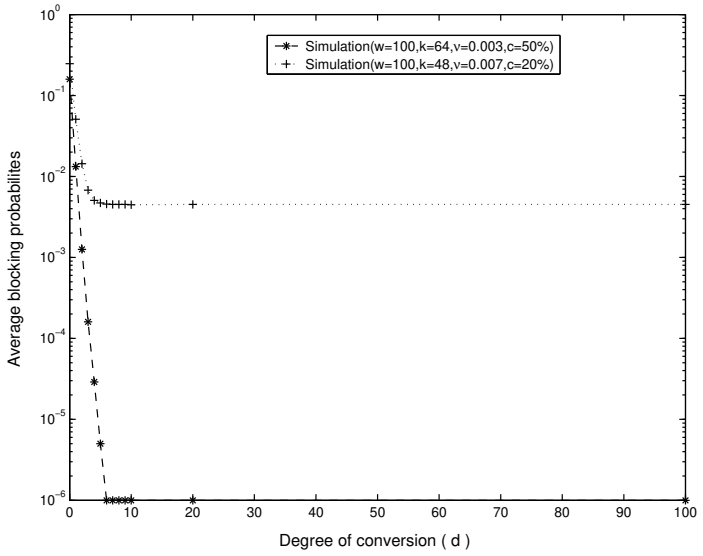

Figure 22: Blocking vs Degree of conversion (d) for large systems

6 Conclusion

In this paper, we proposed an approximate solution for limited-range wavelength conversion in an OBS switch. The problem was modeled as a simultaneous resource possession problem and an approximate product-form solution was proposed. This solution could be applied for very small values of w and d. A method called the four-point method extended the solution for larger values of w. We then proposed a large scale approximation technique which calculated average blocking probabilities for very large values of w and d. d has significant impact on blocking for high percentage of converters available and/or low arrival rate. For small values of partial conversion ($c < w$), the benefits of d saturates very early and large values of d may not be useful. To achieve significantly low blocking of bursts, the utilization has to be kept at very low levels.

References

[1] *GraphPad Prism*. Available at http://www.graphpad.com, 2004.

[2] N. Akar and E. Karasan. Exact calculation of blocking probabilities for bufferless optical burst switched links with partial wavelength conversion. *In Proceedings of Broadnets*, October 2004.

[3] K. Alnowibet and H. Perros. *Nonstationary analysis of circuit-switched communication networks*. Available at http://www.csc.ncsu.edu/faculty/perros/recentpapers.html, 2004.

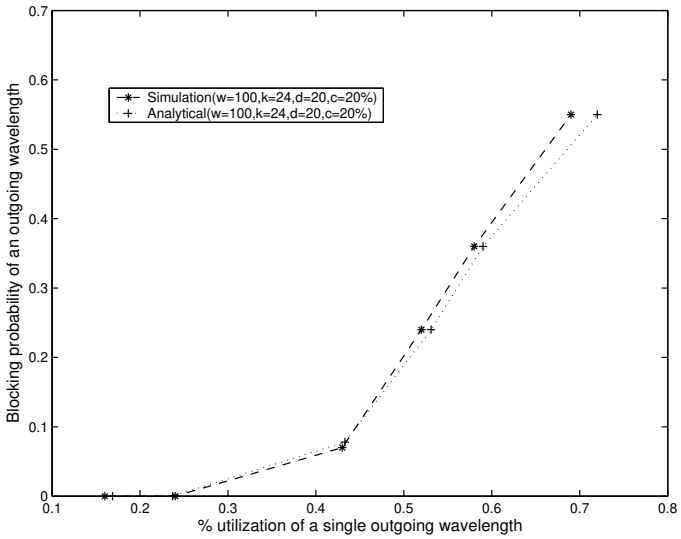

Figure 23: Blocking vs Utilization

[4] L. Battestilli and H. Perros. An introduction to optical burst switching. *IEEE communications magazine*, 41:S10–S15, 2003.

[5] J. Yates, J. Lacey, D. Everitt and M. Summerfield. Limited-range wavelength translation in all-optical networks. *In Proceedings of IEEE INFOCOM*, 3:954–961, March 1996.

[6] C. Gauger. Optimized combination of converter pools and FDL buffers for contention resolution in optical burst switching. *Photonic network communications*, 8:139–148, 2004.

[7] C. Hsu, T. Liu, and N. Huang. Performance analysis of deflection routing in optical burst-switched networks. *In Proceedings of IEEE INFOCOM*, 1:66–73, 2002.

[8] H. Motulsky and A. Christopoulos. *Fitting Models to Biological Data using Linear and Nonlinear Regression: A practical guide to curve fitting.* Available for free download from http://www.curvefit.com/, 2003.

[9] H. G. Perros. *Computer Simulation Techniques: The definitive introduction.* Available for free download from http://www.csc.ncsu.edu/faculty/perros/hp.html, 2004.

[10] I. Baldine, G. Rouskas, H. Perros and D. Stevenson. Jumpstart: a just-in-time signaling architecture for WDM burst-switched networks. *IEEE communications magazine*, 40:82–89, 2002.

[11] V. Puttasubbappa. *Optical Burst Switching: Challenges, Solutions and Performance Evaluation.* PhD thesis, Available at http://www.csc.ncsu.edu/faculty/perros, NCSU, May 2005.

[12] X. Qin and Y. Yang. Nonblocking WDM switching networks with full and limited wavelength conversion. *IEEE Transactions on Communications*, 50:2032–2041, December 2002.

[13] J. Ramamirtham and J.Turner. Design of wavelength converting switches for optical burst switching. *In Proceedings of IEEE INFOCOM*, 1:2032–2041, June 2002.

[14] T. Tripathi and K.N. Sivarajan. Computing approximate blocking probabilities in wavelength routed all-optical networks with limited-range wavelength conversion. *In Proceedings of IEEE INFOCOM*, 1:329–336, March 1999.

[15] Y. Xiong, M. Vandenhoute, and H. Cankaya. Control architecture in optical burst-switched WDM networks. *IEEE Journal on selected areas in communications*, 18:1838–1851, October 2000.

[16] Z. Rosberg, H. Vu and M. Zukerman. Performance evaluation of optical burst switching networks with limited wavelength conversion. *In Proceedings of ONDM 2003, The 7th IFIP Working Conference on Optical Network Design and Modeling*, 2:1155–1169, February 2003.

[17] J.Y. Wei and R.I. McFarland. Just-in-time signaling for WDM optical burst switching networks. *Journal of Lightwave Technology*, 18:2019–2037, December 2000.